Received: 12 August 2019 | Revised: 20 September 2019 | Accepted: 30 September 2019

DOI: 10.1111/cas.14226

ORIGINAL ARTICLE

Cancer Science WILEY

Elevated TRIM23 expression predicts cisplatin resistance in lung adenocarcinoma

Youwei Zhang[1] | He Du[2] | Yang Li[1] | Yuan Yuan[1] | Bi Chen[3] | Sanyuan Sun[1]

[1]Department of Medical Oncology, Xuzhou Central Hospital, Xuzhou Medical University, Xuzhou, China

[2]Department of Medical Oncology, Affiliated Shanghai Pulmonary Hospital, Tongji University, Shanghai, China

[3]Department of Respiratory Medicine, The Affiliated Hospital of Xuzhou Medical University, Xuzhou, China

Correspondence
Bi Chen, Department of Respiratory Medicine, The Affiliated Hospital of Xuzhou Medical University, No. 99 Huaihai West Road, Xuzhou 221002, China.
Email: chenbi207@126.com

Sanyuan Sun, Department of Medical Oncology, Xuzhou Central Hospital, Xuzhou Medical University, No.199 South Jiefang Road, Xuzhou 221009, China.
Email: ss05181@189.cn

Funding information
National Natural Science Foundation of China, Grant/Award Number: 81472615 and 81600044

Abstract

The tripartite motif containing 23 (TRIM23) gene is a member of the tripartite motif (TRIM) family that participates in many pathophysiological processes. However, the role of TRIM23 in lung adenocarcinoma (LUAD) remains unclear. In the present study, TRIM23 was first screened by next-generation sequencing between the cisplatin (DDP)-resistant A549/DDP cell line and the parental A549 cell line, combined with integrated analysis of the Gene Expression Omnibus (GEO) data (E-GEOD-43493 and E-GEOD-43494). The expression of TRIM23 was then verified to be upregulated in the DDP-resistant LUAD cells and tissues. The knockdown of TRIM23 expression in A549/DDP cells caused increased apoptosis, decreased IC_{50} values of DDP, NF-κB nuclear translocation, inhibition of cell proliferation in vitro and in vivo, inhibition of GLUT1/3 expression, glucose uptake, and lactate and ATP production. TRIM23 overexpression resulted in the opposite effects in A549 cells. In addition, the inhibition of proliferation in A549 cells caused by NF-κB signaling inhibitor PTDC or glycolysis inhibitor 3-BrPA could be weakened by TRIM23 overexpression. Furthermore, immunohistochemical analysis revealed that TRIM23 was upregulated in 46.1% (70/152) of LUAD cases, and elevated TRIM23 expression was correlated with high expression of NF-κB, poor cellular differentiation, and adverse overall survival (OS) and disease-free survival (DFS). In conclusion, our study demonstrates that TRIM23 acts as an oncogene in LUAD and promotes DDP resistance by regulating glucose metabolism via the TRIM23/NF-κB/ GLUT1/3 axis.

KEYWORDS
glycolysis, lung adenocarcinoma, NF-κB, resistance, TRIM23

1 | INTRODUCTION

Lung cancer is the leading cause of cancer-related deaths worldwide in both men and women. Lung adenocarcinoma (LUAD) is the fastest growing histological subtype of lung cancer, which develops from small airway epithelial and type II alveolar cells and shows different molecular biology features compared to other types.[1] Although progress has been made in the targeted treatment of LUAD, largely due to the development of small-molecule tyrosine kinase inhibitors (TKI) against epidermal growth factor receptor, anaplastic lymphoma receptor

You-wei Zhang and He Du contributed equally to this work.

tyrosine kinase and c-ros oncogene 1 kinase, platinum-based doublets chemotherapy remains the standard treatment, especially for patients harboring no driving gene alterations or who are resistant to TKI.[2,3] Cisplatin (DDP), which disrupts the structure and function of DNA, is the most commonly used platinum agent for lung cancer.[4] However, resistance to DDP eventually develops and then induces recurrence, invasion and therapeutic failure.[5] Several mechanisms involved in chemoresistance have been revealed, such as decreasing influx or increasing efflux, detoxification by cellular thiols, alteration of drug target and repairing of DNA,[6-8] but these processes are not yet clearly defined. Therefore, an improved understanding of the molecular mechanism of DDP resistance is required for the advancement of LUAD treatment.

Tripartite motif (TRIM)-containing proteins are defined by the presence of an N-terminal RING finger, one or two B-boxes and a coiled-coil (CC) domain. In human beings, approximately 70 TRIM genes have been identified and subdivided based on differences in their C-terminal domains. The RING domain catalyzes ubiquitin chain formation on its substrate through binding to a ubiquitin-conjugating enzyme (E2), suggesting that TRIM proteins serve as E3 ubiquitin ligases. As the process of ubiquitination is responsible for protein quality control, cell cycle regulation, DNA repair and maintaining cell morphology, TRIM family proteins are implicated in various pathophysiological process, including apoptosis, autophagy, immunity, inflammation and carcinogenesis.[9]

Our previous studies have demonstrated a panel of candidate genes that are downregulated by DNA methylation-induced DDP resistance in non-small-cell lung carcinoma using high-throughput microarrays.[10,11] We also found that TRIM23 is significantly upregulated in the resistant A549/DDP cell line compared to the parental A549 cell line, but its specific function is still unclear. Bao et al[12] indicated that TRIM23 mRNA expression is increased in hepatocellular carcinoma (HCC) tissues compared with adjacent normal tissues, and the silencing of TRIM23 by siRNA decreases the motility and invasiveness of HCC cell lines HuH-7 and SK-HEP-1, suggesting an oncogene function of TRIM23. Yao et al (2018) found that elevated TRIM23 expression predicts poor prognosis in gastric cancer.[13] Thus, in the present study, we aimed to further explore the roles of TRIM23 in DDP resistance in LUAD.

2 | MATERIALS AND METHODS

2.1 | Patients

This study enrolled 152 patients who were suffering from primary LUAD and who underwent an operation and received platinum-based doublet adjuvant chemotherapy after surgery at our institutes from 2010 to 2013. None of the patients received preoperative treatment, such as chemotherapy and radiation therapy. The group of patients consisted of 85 men and 67 women, with a median age of 60 (range, 35-80) years. Tumor stage was determined according to the 2017 tumor node metastasis (TNM) classification of malignant tumors by the American Joint Committee on Cancer (AJCC). Cellular differentiation was graded according to the WHO grading system. Overall survival (OS) data were available for all the patients, and patient-free survival (DFS) data were available for 125 patients. The study was carried out in accordance with the approved ethical standards of the ethics committee in our hospitals, and informed consent was obtained from all participants.

2.2 | Cell culture

The human bronchial epithelial cell line 16HBE and LUAD cell line A549 were purchased from Shanghai Institutes for Biological Sciences, Chinese Academy of Cell Resource Center, and were cultured in RPMI 1640 medium (Hyclone) containing 10% FBS and 1% penicillin/streptomycin in a humidified 5% CO_2 incubator at 37°C. The construction and culture of the DDP-resistant A549/DDP cell line were based on our previous study.[11] Primary LUAD cell isolation from fresh tumors, culture and identification of DDP sensitivity have been described previously.[11] In the present study, 50 μmol/L of NF-κB inhibitor pyrrolidine dithiocarbamic acid (PDTC, Sigma-Aldrich) and 20 μmol/L glycolysis inhibitor 3-Bromopyruvate (3-BrPA, Sigma-Aldrich) were used to treat cells.

2.3 | Real-time quantitative PCR

Total RNA was isolated using TRIzol Reagent (Thermo Fisher Scientific). First-strand cDNA was synthesized using 2 μg of total RNA with a reverse transcription kit (TaKaRa). For amplification, cDNA was initially denatured at 95°C for 20 seconds, followed by 40 cycles at 95°C for 5 seconds, and annealing at 60°C for 30 seconds in an ABI 7300 thermocycler (Applied Biosystems) using Power SYBR Green (TaKaRa). The specific primer sequences are designed using Primer Premier 5.0 (www.premierbiosoft.com). The relative expression levels of the genes were calculated using the $2^{-\Delta\Delta Ct}$ method.

2.4 | Lentivirus infection

Lentiviral vector (pLKO.1, Addgene)-meditated small interfering RNA siRNA1-3 were designed and manufactured by GenePharma to knock down TRIM23. The open reading frame of TRIM23 generated by PCR was inserted into the pLVX lentivirus vector (Clontech). These recombinant vectors or negative control (NC) vectors, with psPAX2 and pMD2G packaging vectors (Addgene), were transfected into 293T cells. Three days later, virus supernatants were collected, filtered through 0.45 μm filters, and then subjected to infecting A549 cells or A549/DDP cells. Experimental details are listed in Appendix S1.

2.5 | Western blotting

Nuclear protein and cytoplasmic protein were isolated using a Nuclear and Cytoplasmic Protein Extraction Kit (Beyotime). Cell

protein lysates were separated by 10% SDS-PAGE onto a PVDF membrane (Roche Diagnostics). After soaking the membrane in 10 mL of 5% nonfat milk in Tris-buffered saline with Tween 20 solution for 1 hour, the membrane was incubated with primary antibodies specific to TRIM23, cleaved caspase 3, glucose transporter 1 (GLUT1), GLUT3, nuclear factor-κB (NF-κB), GAPDH and H3 (Univ-bio, Shanghai, China). HRP-conjugated goat antirabbit IgG was used as a secondary antibody. The results were observed following a treatment with an enhanced chemiluminescent (ECL) substrate (Merck Millipore).

2.6 | Gene set enrichment analysis

Gene set enrichment analysis was performed with the JAVA program (http://software.broadinstitute.org/gsea/index.jsp) using MSigDB C2 CP (Canonical pathways) gene set collection. In this study, gene set enrichment analysis (GSEA) first generated an ordered list of all genes according to their correlation with TRIM23 expression, and then a predefined gene set (signature of gene expression upon perturbation of certain cancer-related genes) receives an enrichment score (ES), which is a measure of statistical evidence rejecting the null hypothesis that its members are randomly distributed in the ordered list. Parameters used for the analysis were as follows. The "c2.all.v5.0.symbols.gmt" gene sets were used for running GSEA and 1000 permutations were used to calculate the *P*-value; the permutation type was set to gene_set. The maximum gene set size was fixed at 1500 genes, and the minimum size fixed at 15 genes. The expression level of TRIM23 was used as a phenotype label, and "metric for ranking genes" was set to Pearson correlation. All other basic and advanced fields were set to default.

2.7 | Cell viability and proliferation analysis

Cell viability was assessed using a cell counting kit-8 (CCK-8) assay. Briefly, cells were seeded into 96-well plates at an initial density of 2×10^3 cells/well for 1-3 days. Then, 90 μL of fresh serum-free medium and 10 μL of CCK-8 reagent (Beyotime) were added to each well after decanting the old medium, and the culture was continued at 37°C for 1 hour. The optical density was determined by scanning with a microplate reader (Promega) at a wavelength of 450 nm. IC_{50} values were calculated with a DDP concentration-response curve (concentration gradient: 0, 2, 5, 10 and 20 μg/mL for a 48-hour treatment period) using GraphPad Prism 5.0 (GraphPad Software).

2.8 | Flow cytometry for cell apoptosis

Cells were harvested directly or 48 hours after transfection and washed with ice-cold PBS. The annexin V-FITC apoptosis detection kits (Keygene Biotech) were used to detect cell apoptosis in a FACScan instrument (Becton Dickinson).

2.9 | Metabolite analysis

Cells were seeded into six-well plates (2×10^5 cells/well) and cultured for 6 hours. The culture medium was collected to measure lactate concentrations with a lactic acid assay kit (Jiancheng Bioengineering Institute), after protein quantification (BCA assay). Cellular ATP production was determined using the ATP Assay Kit (Jiancheng Bioengineering Institute). Glucose uptake was detected with a 2-NBDG Glucose Uptake Assay Kit (Cell-Based, AmyJet Scientific Inc) according to the manufacturer's protocol; the fluorescence intensity of 2-NBDG in the cells was recorded using a FACScan instrument (Becton Dickinson).

2.10 | In vivo xenograft model

Six-week-old male BALB/c nude mice were purchased from the Laboratory Animal Center of Nanjing Medical University and maintained under pathogen-free conditions. Tumor xenografts were established by subcutaneous injection of 0.1 mL suspension of cells (2×10^6 cells/mL) into nude mice on the right side of the posterior flank (n = 6 mice per group). Tumor growth was examined every 3 days. After 5-7 days, the tumor volume grew to approximately 100 mm^3, and the mice were intraperitoneally injected with a suspension of PBS containing DDP (2.5 mg/kg) twice per week. The xenograft tumors were harvested and sliced after 4 weeks. Then TUNEL assay kits (Beyotime) were used to analyze apoptosis in situ based on the manufacturer's instructions. The entire experimental protocol was conducted in accordance with the guidelines of the local institutional animal care and use committee.

2.11 | Immunohistochemistry

Formalin-fixed paraffin-embedded tissues were sliced consecutively into 4 μm sections, and then subjected to immunohistochemistry analysis. The sections were incubated with TRIM23 (Abcam; 1:400 dilution) and NFκB antibody (Abcam; 1:400 dilution) at 4°C overnight. After washing in PBS, sections were further incubated with HRP-conjugated secondary antibody for 30 minutes at 37°C. Then, substrate-chromogen (DAB) solution was used to incubate the tumor tissues for 10 minutes. Finally, automated hematoxylin was used to counterstain the slides for 5 minutes. The immunostaining was microscopically evaluated by two independent pathologists. A semiquantitative scoring system was based on the staining intensity and proportion of positive cells.[14]

2.12 | Statistical analysis

SPSS version 16.0 (SPSS) was used for statistical analysis. $P < .05$ was considered statistically significant. The data are presented as

the mean ± standard error. Differences between groups were analyzed using Student's *t* test for comparisons between two groups or one-way analysis of variance for comparisons between more than two groups. OS and DFS curves were calculated using the Kaplan-Meier method and compared by log-rank testing. We also predicted the prognostic value of TRIM23 through survival database KM-plot (http://www.kmplot.com/).

3 | RESULTS

3.1 | The expression status of TRIM23 in DDP-resistant lung adenocarcinoma cells and tissues

We first analyzed transcriptome differences between the A549/DDP cell line and the parental A549 cell line by next-generation sequencing. Using integrated analysis with the GEO data (E-GEOD-43493 and E-GEOD-43494), six TRIM family members were screened and found to be significantly upregulated in A549/DDP cells (Table S1), then were verified by quantified PCR (Figure S1). The most significantly upregulated member, TRIM23, was selected for subsequent experiments. The expression status of TRIM23 in 16HBE, A549 and A549/DDP cells was increased gradually, both at mRNA and protein level (Figure 1A). Using primary tumor cell culture and drug susceptibility testing, 20 LUAD samples were considered DDP-sensitive samples (IC50 < 5 μg/mL), and 20 samples were considered DDP-resistant samples (IC50 > 10 μg/mL). The results showed that the expression levels of TRIM23 were also upregulated in the DDP-resistant tissues (Figure 1B).

3.2 | In vitro effects of TRIM23 expression in DDP resistance

To study the role of TRIM23 in regulating DDP resistance, we used specific siRNA to knock down TRIM23 expression in A549/DDP cells, and TRIM23 overexpressed vectors were transfected into A549 cells (Figure 1C). Gene set enrichment analysis showed that high expression of TRIM23 is negatively correlated with the REACTOME_APOPTOSIS gene set (ES = −0.44658858, *P* = 0, FDR = 0) and is positively correlated with the DACOSTA_UV_RESPONSE_VIA_ERCC3_XPCS_DN gene set (ES = 0.6228651, *P* = 0, FDR = 0) (Figure 1D), indicating that TRIM23 overexpression induced apoptosis resistance and DNA repair. As NFKB1 is listed in the DACOSTA_UV_RESPONSE_VIA_ERCC3_XPCS_DN gene set (Table S2), TRIM23 overexpression may contribute to NF-κB activation. Functional experiments were performed to verify these hypotheses. The knockdown of TRIM23 expression that caused apoptosis increased significantly in A549/DDP cells, with or without DDP treatment (Figure 2A). The concentration of the DDP used in vitro was 10 μmol/L (3 μg/mL). TRIM23 knockdown in A549/DDP cells also caused the IC_{50} values of DDP to decrease and the cell proliferation to be significantly inhibited (Figure 2B). Conversely, the overexpression of TRIM23 resulted in significant inhibition of apoptosis in A549 cells treated with DDP (Figure 2A). TRIM23 overexpression

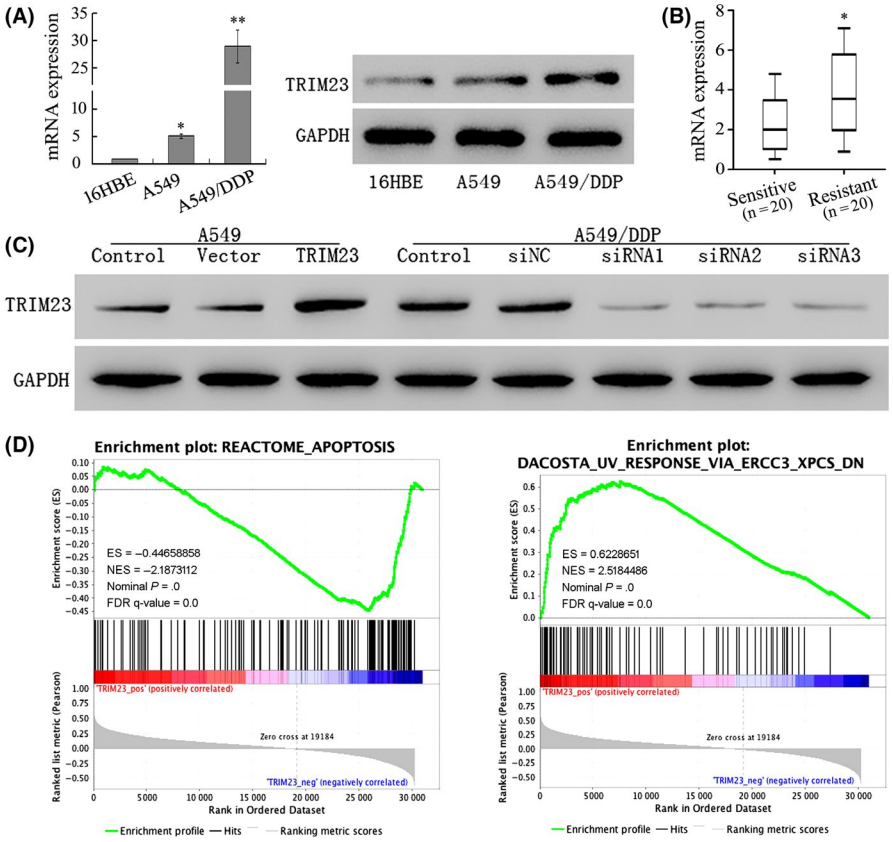

FIGURE 1 The expression status of TRIM23 in cisplatin (DDP)-resistant lung adenocarcinoma cell lines and tissues. (A) The expression status of TRIM23 in the human bronchial epithelial cell line 16HBE, lung adenocarcinoma (LUAD) cell line A549, and DDP-resistant cell line A549/DDP was increased gradually, both at mRNA and protein level. **P* < .05 vs 16HBE; ***P* < .01 vs A549 (B) The TRIM23 expression was analyzed in primary tumor cells; 20 LUAD samples were considered DDP-sensitive samples (IC_{50} < 5 mg/L), and 20 samples were considered DDP-resistant samples (IC_{50} > 10 mg/L) **P* < .05 (C) Lentiviral vector-meditated siRNA to knock down TRIM23 expression in A549/DDP cells, and TRIM23 overexpressed vector were transfected into A549 cells. (D) Gene set enrichment analysis (GSEA) showed that high expression of TRIM23 was negatively correlated with the REACTOME_APOPTOSIS gene set and is positively correlated with the DACOSTA_UV_RESPONSE_VIA_ERCC3_XPCS_DN gene set

also increased IC_{50} values of DDP and increased proliferation of A549 cells (Figure 2C). In addition, the inhibition of proliferation in A549 cells caused by NF-κB signaling inhibitor PTDC could be weakened by TRIM23 overexpression (Figure 2C), suggesting that TRIM23 may function by activating NF-κB signaling.

3.3 | TRIM23 promotes DDP resistance by regulating glucose metabolism

Western blot analysis showed that knockdown of TRIM23 in A549/DDP cells caused a significant upregulation of cleaved caspase 3, and an inhibition of GLUT1/3 expression and NF-κB nuclear translocation, while TRIM23 overexpression in A549 cells caused the opposite effects (Figure 3A). In A549 cells, PTDC treatment also induced significant upregulation of cleaved caspase 3 and inhibition of GLUT1/3 expression and NF-κB nuclear translocation; the overexpression of TRIM23 could counteract these effects (Figure 3A). Therefore, NF-κB signaling and glycolysis were closely associated with TRIM23; glucose metabolism was analyzed subsequently. Knockdown of TRIM23 in A549/DDP cells significantly inhibited glucose uptake, and lactate and ATP production, while overexpression of TRIM23 in A549 cells significantly increased glucose uptake, and lactate and ATP production (Figure 3B). Similarly, PTDC treatment inhibited glucose metabolism in A549 cells, and the overexpression of TRIM23 counteracted these effects (Figure 3B). Moreover, TRIM23 overexpression weakened the proliferation inhibition of A549 cells by glycolysis inhibitor 3-BrPA (Figure 2C). These results indicate that TRIM23 promotes DDP resistance in vitro by regulating glucose metabolism via NF-κB activation.

3.4 | In vivo effects of TRIM23 expression in DDP resistance

The effects of TRIM23 on DDP chemotherapeutic sensitivity in vivo were then investigated. All the xenograft models were treated with DDP. As shown in Figure 4A,B, TRIM23 knockdown significantly inhibited xenograft growth in mice inoculated with A549/DDP cells, while

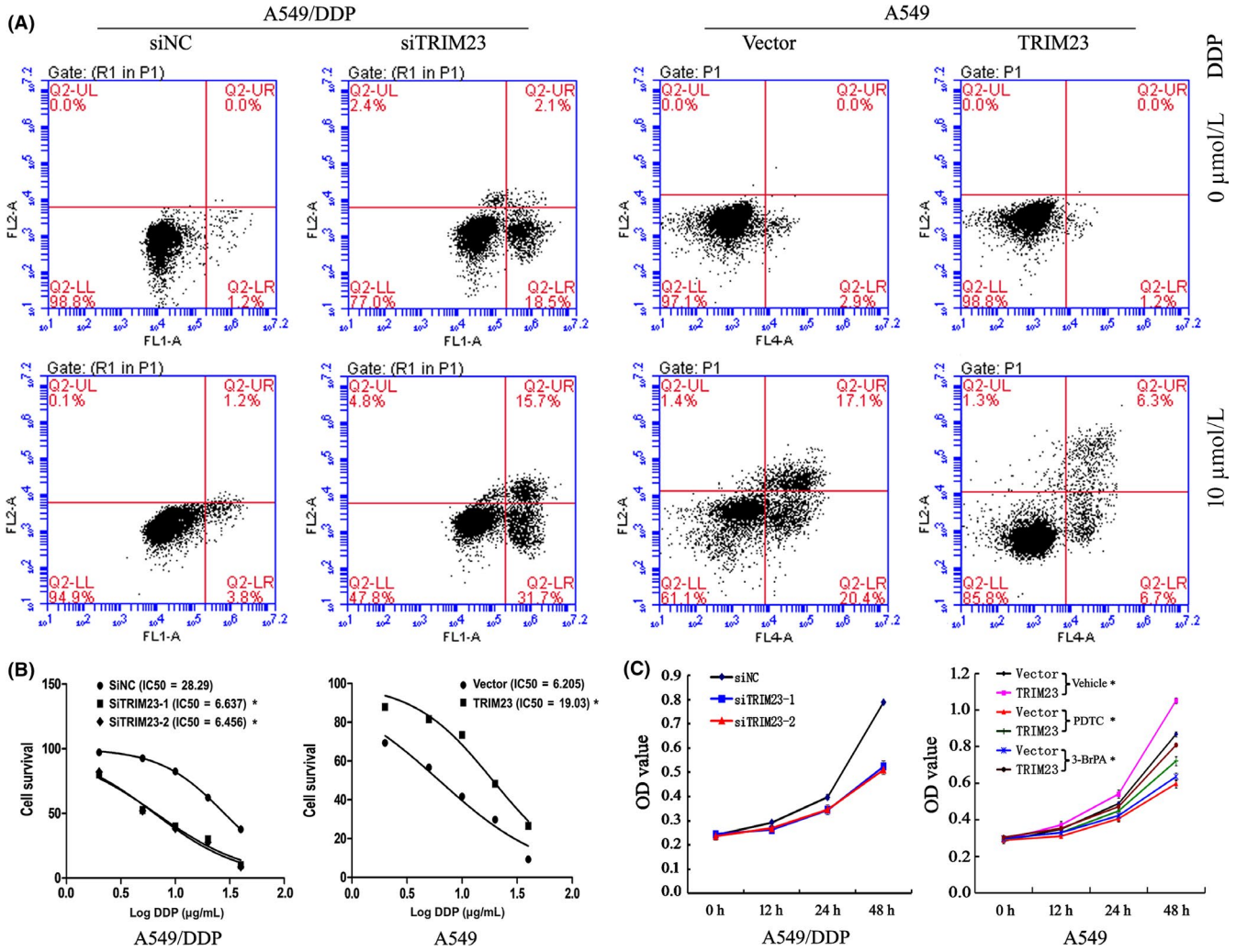

FIGURE 2 In vitro effects of TRIM23 expression in DDP resistance. (A) Cell apoptosis was evaluated by flow cytometry, before and after 10 μmol/L DDP treatment. Using a CCK-8 assay, the IC_{50} values of DDP were calculated (B), and cell proliferation was analyzed (C). PDTC, a NF-κB inhibitor pyrrolidine dithiocarbamic acid; 3-BrPA, a glycolysis inhibitor 3-Bromopyruvate; *$P < .05$ vs control

the overexpression of TRIM23 increased xenograft growth in mice inoculated with A549 cells. TUNEL analysis of tumor tissues further revealed significantly increased apoptosis cells in tumors derived from TRIM23 knockdown A549/DDP cells compared with mock cells, and decreased apoptosis in tumors derived from TRIM23 overexpression A549 cells (Figure 4C), indicating that TRIM23 knockdown enhances DDP cytotoxicity and TRIM23 overexpression promotes DDP resistance in vivo.

3.5 | Elevated TRIM23 expression predicts poor prognosis

To better understand the association of TRIM23 expression and DDP resistance, the protein expression levels of TRIM23 and NF-κB were assessed in 152 patients diagnosed with LUAD and treated with platinum-based adjuvant chemotherapy. Immunohistochemical analysis revealed that TRIM23 was upregulated (high expression, score ≧3) in 70 cases (46.1%), and elevated TRIM23 expression was correlated with high expression of NF-κB (Figure 5A,B). Moreover, TRIM23 protein expression was significantly associated with poor cellular differentiation but not correlated with patients' gender, age, size, lymph metastasis and clinical stage (Table 1).

By the end of the follow-up period, a total of 88 patients had died within 6 years after surgery. Univariate survival analysis showed that patients with high expression of TRIM23 were associated with shorter OS than those with low expression (mean 54.13 months (95% CI 46.60-61.65) versus 66.98 months [95% CI 59.72-74.25], $P = .040$) (Figure 5C). Among the 125 patients for whom we had DFS

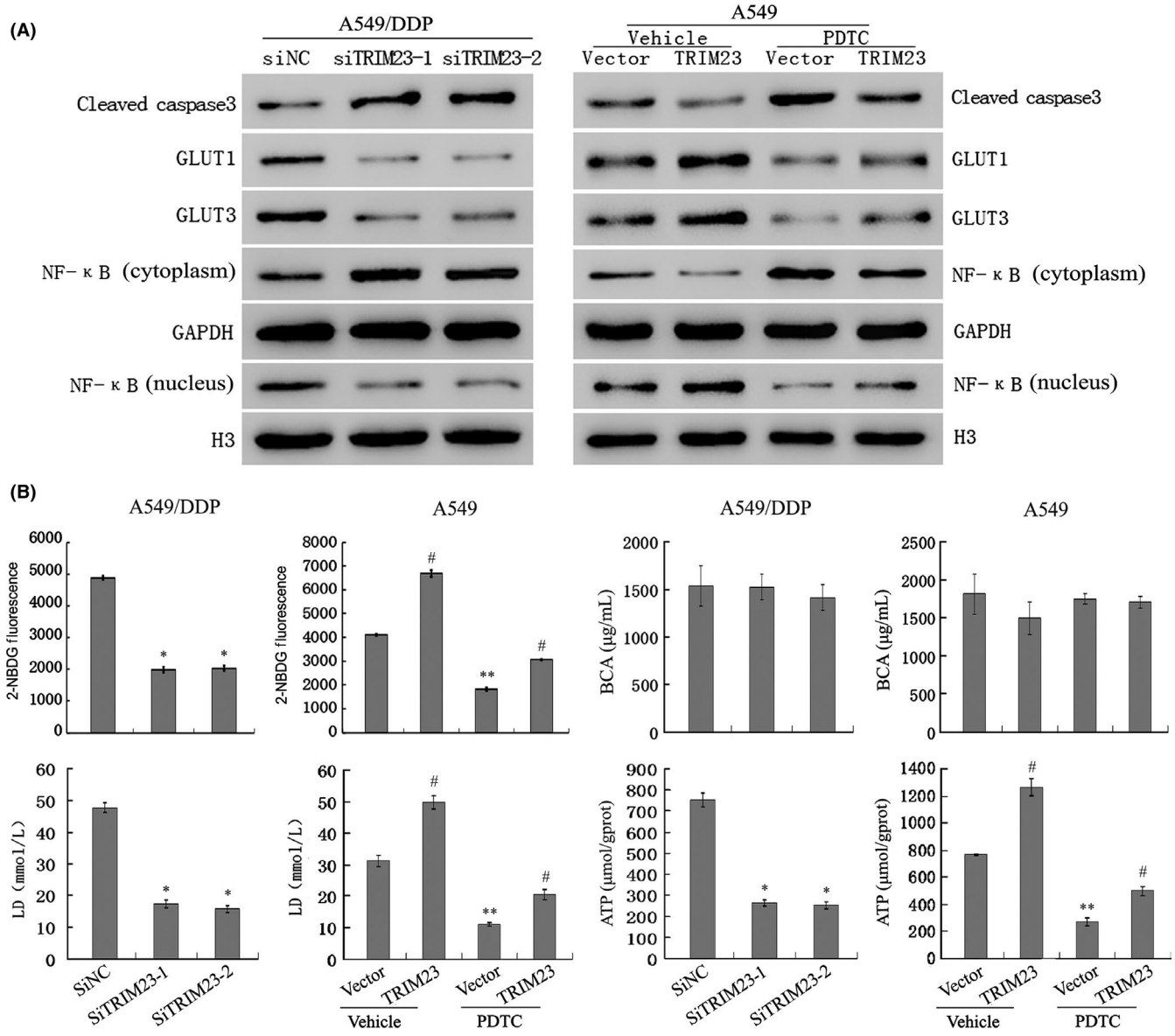

FIGURE 3 TRIM23 promotes DDP resistance by regulating glucose metabolism. (A) Western blot analysis of the protein expression levels in A549/DDP cells with TRIM23 knockdown and in A549 cells with TRIM23 overexpression and/or PTDC treatment. (B) Glucose uptake, lactate and ATP production were analyzed in A549/DDP cells with TRIM23 knockdown and in A549 cells with TRIM23 overexpression and/or PTDC treatment. *$P < .05$ vs siNC; **$P < .05$ vs vehicle; #$P < .05$ vs vector

data, TRIM23 high expression showed an inferior DFS compared to those with low expression (mean 34.60 months [95% CI 29.09-40.11] vs 46.14 months [95% CI 39.34-52.94], $P = .019$) (Figure 5D). Multivariate survival analysis from the KM-plot database further verified that LUAD patients with high expression of TRIM23 mRNA were associated with shorter OS than those with low expression (Hazard Ratio [HR] = 1.4, $P = .0045$) (Figure 5E). These data suggest that TRIM23 may affect LUAD prognosis and platinum resistance by activating NF-κB.

4 | DISCUSSION

The tripartite motif family proteins may act as oncogenes or tumor suppressor genes in different types of malignancies. For example, TRIM44 expression is significantly upregulated in human esophageal cancer (HEC) tissues and promotes HEC development by epithelial-mesenchymal transition (EMT) via the AKT/mTOR pathway,[15] whereas TRIM50 suppresses hepatocarcinoma progression through directly targeting SNAIL for ubiquitous degradation.[16] However, the studies on TRIM23 in tumors are not sufficient. In the present study, we first found that TRIM23 was upregulated in the DDP-resistant LUAD cells and tissues, and elevated TRIM23 expression was associated with poor cellular differentiation and adverse prognosis in LUAD patients treated with platinum-based adjuvant chemotherapy, implying that TRIM23 promotes LUAD development and DDP resistance. Functional experiments in vitro and in vivo confirmed that TRIM23 acts as an oncogene in LUAD, which was consistent with results in previous reports.[12,13]

The mechanism of TRIM23 has been explored in different fields. Watanabe et al[17] found that TRIM23 regulates adipocyte differentiation through stabilization of the adipogenic activator peroxisome proliferator-activated receptor γ (PPARγ). Sparrer et al[18] found that TRIM23 mediates virus-induced autophagy via activation of TANK-binding kinase 1 (TBK1). Furthermore, TRIM23 plays important roles in the regulation of NF-κB signaling in antiviral defense.[19,20] In an HCC model, miR-194 suppresses the migration and invasion of cancer cells by targeting C21ORF91 and TRIM23; knocking down either protein decreased the activity of a luciferase NF-κB reporter.[12] Thus, NF-κB activation may be a crucial downstream signaling pathway for TRIM23 overexpression. NF-κB signaling is activated by various cell surface or intracellular receptors. The tripartite motif23 may interact with these cytokines to positively regulate NF-κB signaling. Recent studies have suggested that TRIM family proteins play a critical role in regulation of the NF-κB pathway by ubiquitinating proteins at different steps.[21-23] We performed GSEA analysis and found that high expression of

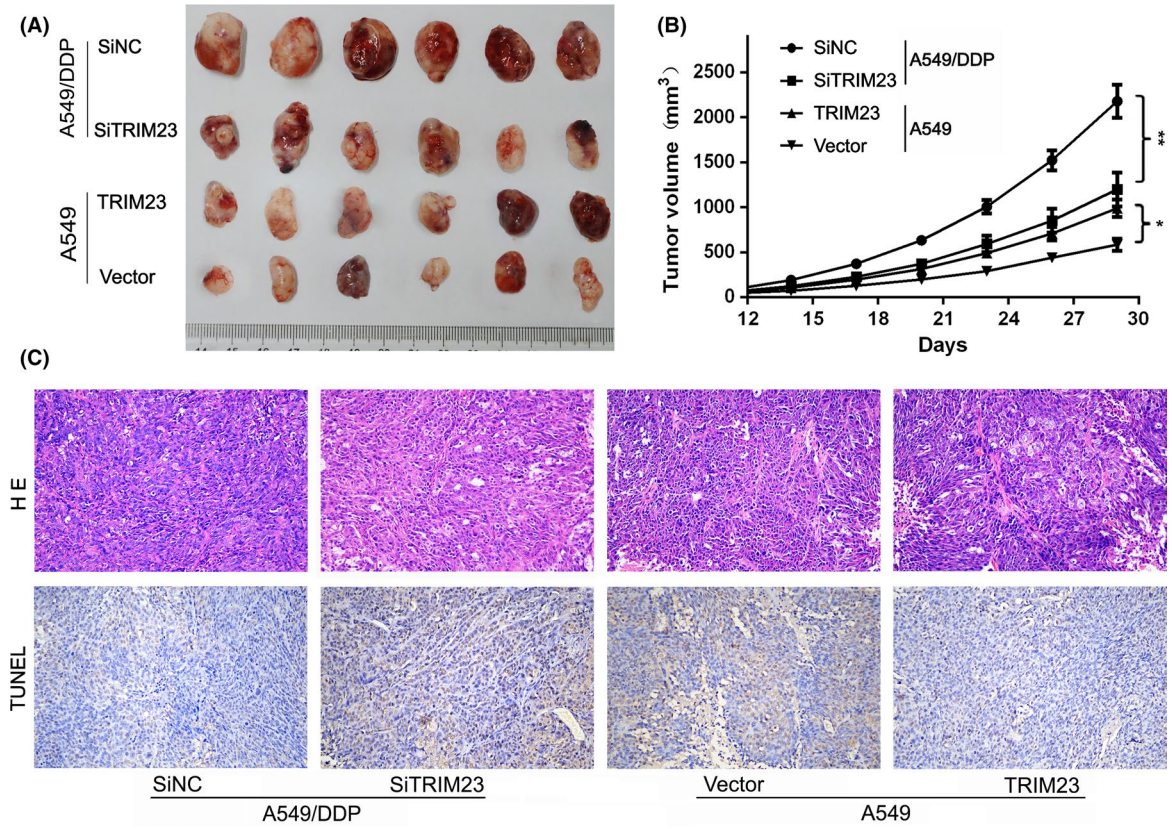

FIGURE 4 In vivo effects of TRIM23 expression in DDP resistance. Cells (2×10^6 cells/100 μL PBS) were subcutaneously inoculated into the right flank of BALB/c nu/nu mice, and the animals were randomly separated into four groups (six per group) according to the inoculated cells. The mice were intraperitoneally injected with a suspension of PBS containing DDP (2.5 mg/kg) twice per week, after the tumor volume grew to approximately 100 mm^3. (A) The mice were killed, and the tumors were isolated after 4 wk. (B) The tumor size was monitored every 3 d after cell implantation. (C) Apoptosis in situ was detected by TUNEL assay. *$P < .05$ vs vector; **$P < .01$ vs SiNC

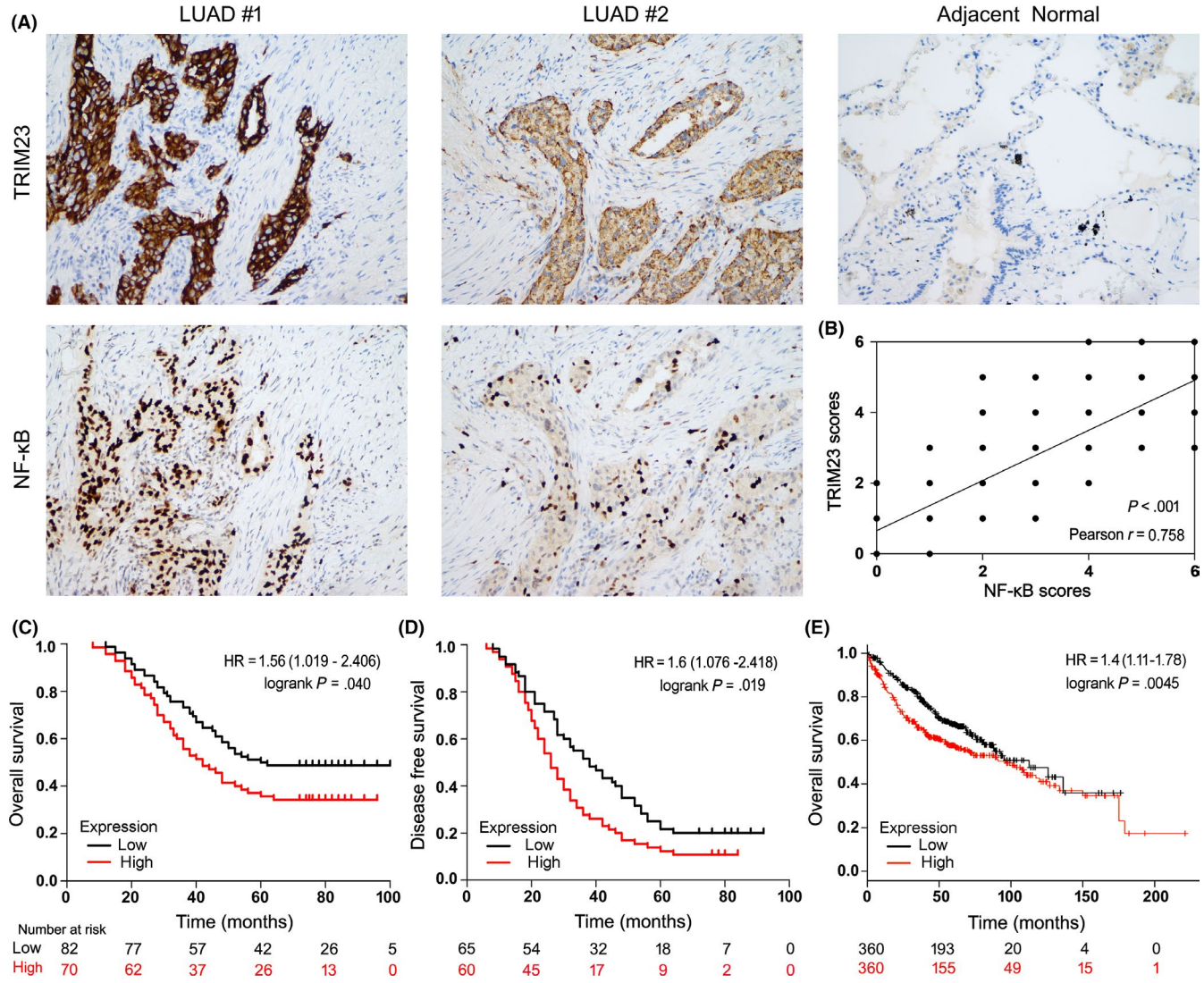

FIGURE 5 Elevated TRIM23 expression predicts poor prognosis. (A) TRIM23 and NF-κB expression in LUAD tissues and adjacent normal tissues determined by immunohistochemical staining in serial sections (EnVision, magnification × 200). (B) Relationship between TRIM23 and NF-κB expression in tumors. Univariate survival analysis showed that patients with high expression of TRIM23 protein were associated with adverse overall survival (OS) (C) and disease-free survival (DFS) (D) compared to those with low expression. (E) Multivariate survival analysis from the KM-plot database verified that LUAD patients with high expression of TRIM23 mRNA were associated with shorter OS than those with low expression

TRIM23 was correlated with apoptosis resistance and DNA repair. As expected, NFKB1 is a member of the DNA repair gene set, and elevated TRIM23 expression in LUAD tissues is correlated with high expression of NF-κB. The functional experiments further verified that TRIM23 promotes DDP resistance in LUAD by activating NF-κB signaling.

Constitutive activation of the proinflammatory transcription factor NF-κB has been found to play important roles in progression of lung carcinoma and DDP resistance.[24-26] NF-κB is present in the cytoplasm bound to NF-κB inhibitor (IκB), which inhibits the nuclear translocation of NF-κB. However, phosphorylation of IκB by IκB kinase (IKK) releases NF-κB, which then translocates to the nucleus and activates transcription of various genes involved in cellular survival, proliferation and migration. Recently, growing evidence has suggested a link between NF-κB and abnormal glucose metabolism.[27-30] In p53-deficient primary cultured cells, kinase activities of IKKα and IKKβ and subsequent NF-κB activity were enhanced, resulting in an increase of aerobic glycolysis and upregulation of GLUT3. Oncogenic Ras-induced cell transformation and increase of aerobic glycolysis in p53-deficient cells were suppressed in the absence of NF-κB expression, and were restored by GLUT3 expression.[31] Another study found that macrophage migration inhibitory factor (MIF) promotes cell proliferation and aerobic glycolysis in lung cancer, and blocking the NF-κB/HIF-1α signaling pathway largely abolishes the effects of MIF.[32] In the present study, the changes of GLUT1/3 expression and NF-κB nuclear translocation remained consistent after TRIM23 knockdown or overexpression, indicating the significance of the TRIM23/NF-κB/ GLUT1/3 axis in DDP resistance.

TABLE 1 Association between TRIM23 expression in lung adenocarcinoma tissues and clinicopathological features

Characteristics	Number	High expression of TRIM23 n (%)	*P*-value
Gender			
Male	85	40 (47.0)	.779
Female	67	30 (44.8)	
Age			
<60	71	32 (45.1)	.938
≥60	81	38 (46.9)	
Tumor size			
>3 cm	67	34 (50.7)	.303
≤3 cm	85	36 (42.4)	
Differentiation			
Well/Moderate	102	41 (40.2)	.039*
Poor	50	29 (58.0)	
Lymph metastasis			
No	81	34 (42.0)	.281
Yes	71	36 (50.7)	
Stage			
I/II	68	27 (39.7)	.158
III/IV	84	43 (51.2)	

*$P < .05$

Aberrant metabolism is considered as one of the essential characteristics of malignancy. Cancer cells preferentially metabolize glucose through glycolysis even in the presence of sufficient oxygen and this phenomenon has been referred to as aerobic glycolysis or the Warburg effect,[33,34] which provides the cancer cell with ATP in a less efficient manner than oxidative phosphorylation. However, the cancer cell benefits because glycolysis also provides substrates for anabolic processes; it is believed to offer a selective advantage for the proliferation and survival.[35] An extremely high rate (up to 200-fold) of glycolysis is always detected in cancer cells, as compensation for the inefficiency of energy generation.[36] This enhancement of glucose metabolism requires an accelerated glucose uptake into cancer cells. A family of glucose transporter proteins (GLUT) facilitates the glucose transport across the plasma membranes of mammalian cells in a tissue-specific manner. Until now, 14 different GLUT isoforms have been identified.[37] Both GLUT1 and GLUT3 are reported to be associated with lung cancer progression.[38,39] In our study, knockdown of TRIM23 in A549/DDP cells significantly inhibited glucose uptake, and lactate and ATP production, while TRIM23 overexpression in A549 cells increased glucose uptake, and lactate and ATP production. Therefore, the role of the TRIM23/NF-κB/GLUT1/3 axis in LUAD may be achieved by regulating glucose metabolism.

Overall, our study demonstrates that TRIM23 acts as an oncogene in LUAD and promotes DDP resistance by regulating glucose metabolism via the TRIM23/NF-κB/GLUT1/3 axis, providing new insight into the mechanisms underlying the TRIM family and contributing to treatment of LUAD patients with platinum resistance.

ACKNOWLEDGMENTS

This study was funded by the National Natural Science Foundation of China (grant numbers: 81472615 and 81600044).

DISCLOSURE

The authors declare no conflicts of interest for this article.

ORCID

Bi Chen https://orcid.org/0000-0002-6041-6433
Sanyuan Sun https://orcid.org/0000-0002-7477-7491

REFERENCES

1. Denisenko TV, Budkevich IN, Zhivotovsky B. Cell death-based treatment of lung adenocarcinoma. *Cell Death Dis*. 2018;9:117.
2. Wen M, Xia J, Sun Y, et al. Combination of EGFR-TKIs with chemotherapy versus chemotherapy or EGFR-TKIs alone in advanced NSCLC patients with EGFR mutation. *Biologics*. 2018;12:183-190.
3. Lee SH. Chemotherapy for lung cancer in the era of personalized medicine. *Tuberc Respir Dis (Seoul)*. 2019;82:179-189.
4. Fennell DA, Summers Y, Cadranel J, et al. Cisplatin in the modern era: the backbone of first-line chemotherapy for non-small cell lung cancer. *Cancer Treat Rev*. 2016;44:42-50.
5. Amable L. Cisplatin resistance and opportunities for precision medicine. *Pharmacol Res*. 2016;106:27-36.
6. Ishida S, McCormick F, Smith-McCune K, Hanahan D, et al. Enhancing tumor-specific uptake of the anticancer drug cisplatin with a copper chelator. *Cancer Cell*. 2010;17:574-583.
7. Chen HH, Kuo MT. Role of glutathione in the regulation of Cisplatin resistance in cancer chemotherapy. *Met Based Drugs*. 2010;2010:430939.
8. Yu WK, Wang Z, Fong CC, et al. Chemoresistant lung cancer stem cells display high DNA repair capability to remove cisplatin-induced DNA damage. *Br J Pharmacol*. 2017;174:302-313.
9. Hatakeyama S. TRIM family proteins: roles in autophagy, immunity, and carcinogenesis. *Trends Biochem Sci*. 2017;42:297-311.
10. Zhang Y, Yuan Y, Li Y, Zhang P, Chen P, Sun S. An inverse interaction between HOXA11 and HOXA11-AS is associated with cisplatin resistance in lung adenocarcinoma. *Epigenetics*. 2019;14:949-960.
11. Zhang YW, Zheng Y, Wang JZ, et al. Integrated analysis of DNA methylation and mRNA expression profiling reveals candidate genes associated with cisplatin resistance in non-small cell lung cancer. *Epigenetics*. 2014;9:896-909.
12. Bao C, Li Y, Huan L, et al. NF-κB signaling relieves negative regulation by miR-194 in hepatocellular carcinoma by suppressing the transcription factor HNF-1α. *Sci Signal*. 2015;8:ra75.
13. Yao Y, Liu Z, Guo H, et al. Elevated TRIM23 expression predicts poor prognosis in Chinese gastric cancer. *Pathol Res Pract*. 2018;214:2062-2068.
14. Deng W, Jiao N, Li N, Wan X, Luo S, Zhang Y. Decreased expression of PinX1 protein predicts poor prognosis of colorectal cancer patients receiving 5-FU adjuvant chemotherapy. *Biomed Pharmacother*. 2015;73:1-5.
15. Xiong D, Jin C, Ye X, et al. TRIM44 promotes human esophageal cancer progression via the AKT/mTOR pathway. *Cancer Sci*. 2018;109:3080-3092.
16. Ma X, Ma X, Qiu Y, et al. TRIM50 suppressed hepatocarcinoma progression through directly targeting SNAIL for ubiquitous degradation. *Cell Death Dis*. 2018;9:1029.

17. Watanabe M, Takahashi H, Saeki Y, et al. The E3 ubiquitin ligase TRIM23 regulates adipocyte differentiation via stabilization of the adipogenic activator PPARγ. *Elife*. 2015;4:e05615.
18. Sparrer KMJ, Gableske S, Zurenski MA, et al. TRIM23 mediates virus-induced autophagy via activation of TBK1. *Nat Microbiol*. 2017;2:1543-1557.
19. Arimoto K, Funami K, Saeki Y, et al. Polyubiquitin conjugation to NEMO by triparite motif protein 23 (TRIM23) is critical in antiviral defense. *Proc Natl Acad Sci U S A*. 2010;107:15856-15861.
20. Poole E, Groves I, MacDonald A, Pang Y, Alcami A, Sinclair J. Identification of TRIM23 as a cofactor involved in the regulation of NF-kappaB by human cytomegalovirus. *J Virol*. 2009;83:3581-3590.
21. Tomar D, Singh R. TRIM family proteins: emerging class of RING E3 ligases as regulator of NF-κB pathway. *Biol Cell*. 2015;107:22-40.
22. Yang W, Liu L, Li C, et al. TRIM52 plays an oncogenic role in ovarian cancer associated with NF-kB pathway. *Cell Death Dis*. 2018;9:908.
23. Luo Q, Lin H, Ye X, Huang J, Lu S, Xu L. Trim44 facilitates the migration and invasion of human lung cancer cells via the NF-κB signaling pathway. *Int J Clin Oncol*. 2015;20:508-517.
24. Zakaria N, Mohd Yusoff N, Zakaria Z, Widera D, Yahaya BH. Inhibition of NF-κB signaling reduces the stemness characteristics of lung cancer stem cells. *Front Oncol*. 2018;8:166.
25. Li Y, He LR, Gao Y, et al. CHD1L contributes to cisplatin resistance by upregulating the ABCB1-NF-κB axis in human non-small-cell lung cancer. *Cell Death Dis*. 2019;10:99.
26. Shen W, Qiu Y, Li J, et al. IL-25 promotes cisplatin resistance of lung cancer cells by activating NF-κB signaling pathway to increase of major vault protein. *Cancer Med*. 2019;8:3491-3501.
27. Johnson RF, Perkins ND. Nuclear factor-κB, p53, and mitochondria: regulation of cellular metabolism and the Warburg effect. *Trends Biochem Sci*. 2012;37:317-324.
28. Zhou J, Li Y, Li D, Liu Z, Zhang J. Oncoprotein LAMTOR5 activates GLUT1 via upregulating NF-κB in liver cancer. *Open Med (Wars)*. 2019;14:264-270.
29. Jiao L, Wang S, Zheng Y, et al. Betulinic acid suppresses breast cancer aerobic glycolysis via caveolin-1/NF-κB/c-Myc pathway. *Biochem Pharmacol*. 2019;161:149-162.
30. Park SY, Shin JH, Kee SH. E-cadherin expression increases cell proliferation by regulating energy metabolism through nuclear factor-κB in AGS cells. *Cancer Sci*. 2017;108:1769-1777.
31. Kawauchi K, Araki K, Tobiume K, Tanaka N. p53 regulates glucose metabolism through an IKK-NF-kappaB pathway and inhibits cell transformation. *Nat Cell Biol*. 2008;10:611-618.
32. Li J, Zhang J, Xie F, Peng J, Wu X. Macrophage migration inhibitory factor promotes Warburg effect via activation of the NF κB/HIF 1α pathway in lung cancer. *Int J Mol Med*. 2018;41:1062-1068.
33. Vander Heiden MG, Cantley LC, Thompson CB. Understanding the Warburg effect: the metabolic requirements of cell proliferation. *Science*. 2009;324:1029-1233.
34. Vaupel P, Schmidberger H, Mayer A. The Warburg effect: essential part of metabolic reprogramming and central contributor to cancer progression. *Int J Radiat Biol*. 2019;95:912-919.
35. Elf SE, Chen J. Targeting glucose metabolism in patients with cancer. *Cancer*. 2014;120:774-780.
36. Akram M. Mini-review on glycolysis and cancer. *J Cancer Educ*. 2013;28:454-457.
37. Ancey PB, Contat C, Meylan E. Glucose transporters in cancer - from tumor cells to the tumor microenvironment. *FEBS J*. 2018;285:2926-2943.
38. Zhang B, Xie Z, Li B. The clinicopathologic impacts and prognostic significance of GLUT1 expression in patients with lung cancer: a meta-analysis. *Gene*. 2019;689:76-83.
39. Masin M, Vazquez J, Rossi S, et al. GLUT3 is induced during epithelial-mesenchymal transition and promotes tumor cell proliferation in non-small cell lung cancer. *Cancer Metab*. 2014;2:11.

SUPPORTING INFORMATION

Additional supporting information may be found online in the Supporting Information section.

How to cite this article: Zhang Y, Du H, Li Y, Yuan Y, Chen B, Sun S. Elevated TRIM23 expression predicts cisplatin resistance in lung adenocarcinoma. *Cancer Sci*. 2020;111:637–646. https://doi.org/10.1111/cas.14226